INTERNATIONAL JOURNAL FOR NUMERICAL METHODS IN FLUIDS, VOL. 10, 141–160 (1990)

FINITE ELEMENT SOLUTIONS OF AXISYMMETRIC EULER EQUATIONS FOR AN INCOMPRESSIBLE AND INVISCID FLUID

JACQUES-HERVE SAIAC

CNAM,-INRIA, Domaine de Voluceau-Rocquencourt, B.P. 105-78153, Le Chesnay, Cedex (France)

SUMMARY

In this paper we present a finite element method for the numerical solution of axisymmetric flows. The governing equations of the flow are the axisymmetric Euler equations. We use a streamfunction angular velocity and vorticity formulation of these equations, and we consider the non-stationary and the stationary problems.

For industrial applications we have developed a general model which computes the flow past an annular aerofoil and a duct propeller. It is able to take into account jumps of angular velocity and vorticiy in order to model the flow in the presence of a propeller. Moreover, we compute the complete flow around the after-body of a ship and the interaction between a ducted propeller and the stern. In the stationary case we have developed a simple and efficient version of the characteristics/finite element method. Numerical tests have shown that this last method leads to a very fast solver for the Euler equations. The numerical results are in good agreement with experimental data.

KEY WORDS Inviscid incompressible flows Axisymmetric Finite element Characteristics Ducted propeller

1. INTRODUCTION

The streamfunction and vorticity formulation of the Euler equations governing an incompressible and non-viscous flow has been successfully used in two-dimensional problems. In a finite element context it has been associated with either classical leap-frog or Crank–Nicolson time-differencing schemes[1,2] or with the method of characteristics.[3–6]

It is well known that in the axisymmetric case there is also a streamfunction formulation of the Euler equations. It uses the θ-components, in cylindrical co-ordinates, of the vector potential, the velocity and the vorticity. The choice of this formulation has, in our case, many advantages. Among them we can mention the following.

1. The axisymmetric flow is completely described by three scalar functions.
2. The incompressibility condition is exactly satisfied.
3. From a computational point of view, this formulation gives a simple model leading to fast solvers well adapted to our purpose: 'trial and error' procedures in engineering design.

Our model involve three equations: one elliptic equation for the streamfunction and two transport equations for the angular velocity and the vorticity. A finite element method using non-uniform meshes has been chosen in order to get a general spatial discretization giving a soft treatment of the geometry. Then the main difficulty of the numerical solution of the Euler

0271–2091/90/020141–20$10.00

Received March 1989

equations is to write a good solver for the transport equations. Since for applications in 'pump-jet' design we have to model the convection of jumps of angular velocity and vorticity, we need a robust method, especially well suited to difficult problems with rough conditions. This has been the key point of this work.

One can find in Reference 7 a general review of numerical methods in turbomachinery flows, and in References 8 and 9 some finite element applications. The present work differs from the preceding by the choice of triangular meshes, direct solutions by Choleski factorizations of the elliptic equation and an exact and direct treatment of the Kutta–Joukovski condition, obtained elsewhere through an iterative process. Our final choice of a stationary implementation of the characteristics method to solve the convection problem is the original part of this work.

This paper is organized as follows. In Sections 2 and 3 we derive the mathematical formulations and the boundaries conditions of the problem, and specify the treatment of the Kutta–Joukovski condition. In Section 4 we present the finite element spatial discretization and give a convergence result in a simpler model case without 'swirl'. Section 5 deals with time discretizations using leap-frog and semi-implicit Crank–Nicolson schemes. We derive theoretical stability results in both cases and present some numerical tests showing the inability of this classical approach to model the flow correctly. Sections 6 and 7 are devoted to our implementation of the characteristics method giving the stationary solution of the flow by an iterative fixed-point algorithm. Finally, in Section 8 we present numerical results in the case of the complete model of a duct propeller. They reveal good agreement with experiments carried out by B. Goirand at the Bassin des Carenes in Paris.

2. THE MATHEMATICAL MODEL

The general three-dimensional Euler equations in cylindrical co-ordinates r, θ, z are

$$\frac{\partial V_r}{\partial t} + V_r\frac{\partial V_r}{\partial r} + \frac{V_\theta}{r}\frac{\partial V_r}{\partial \theta} - \frac{V_\theta^2}{r} + V_z\frac{\partial V_r}{\partial z} = -\frac{1}{\rho}\frac{\partial p}{\partial r}, \tag{1a}$$

$$\frac{\partial V_\theta}{\partial t} + V_r\frac{\partial V_\theta}{\partial r} + \frac{V_\theta}{r}\frac{\partial V_\theta}{\partial \theta} + \frac{V_\theta V_r}{r} + V_z\frac{\partial V_\theta}{\partial z} = -\frac{1}{\rho r}\frac{\partial p}{\partial \theta}, \tag{1b}$$

$$\frac{\partial V_z}{\partial t} + V_r\frac{\partial V_z}{\partial r} + \frac{V_\theta}{r}\frac{\partial V_z}{\partial \theta} + V_z\frac{\partial V_z}{\partial z} = -\frac{1}{\rho}\frac{\partial p}{\partial z}, \tag{1c}$$

with

$$\operatorname{div}(V) = \frac{1}{r}\frac{\partial}{\partial r}(rV_r) + \frac{1}{r}\frac{\partial V_\theta}{\partial \theta} + \frac{\partial V_z}{\partial z} = 0, \tag{1d}$$

where V_r, V_θ, V_z are the components of the velocity, ρ is the density of the fluid and p is the pressure. They reduce in the axisymmetric case to the following system.

$$\frac{\partial V_r}{\partial t} + V_r\frac{\partial V_r}{\partial r} + V_z\frac{\partial V_r}{\partial z} = \frac{V_\theta^2}{r} - \frac{1}{\rho}\frac{\partial p}{\partial r}, \tag{2a}$$

$$\frac{\partial V_\theta}{\partial t} + V_r\frac{\partial V_\theta}{\partial r} + V_z\frac{\partial V_\theta}{\partial z} = -\frac{V_\theta V_r}{r}, \tag{2b}$$

$$\frac{\partial V_z}{\partial t} + V_r\frac{\partial V_z}{\partial r} + V_z\frac{\partial V_z}{\partial z} = -\frac{1}{\rho}\frac{\partial p}{\partial z}, \tag{2c}$$

with

$$\frac{1}{r}\frac{\partial}{\partial r}(r V_r)+\frac{\partial V_z}{\partial z}=0. \tag{2d}$$

Remark 1

We do not restrict ourselves to the case $V_\theta = 0$. We just take the derivatives

$$\frac{\partial}{\partial \theta}=0.$$

We introduce a streamfunction ψ_θ such that the meridian velocity

$$V_{\mathrm{M}}=(V_z, V_r)$$

can be written

$$V_z=\frac{1}{r}\frac{\partial(r\psi_\theta)}{\partial r}, \qquad V_r=-\frac{1}{r}\frac{\partial(r\psi_\theta)}{\partial z}. \tag{3}$$

Thus the zero-divergence condition (2d) is automatically satisfied. Now we consider the θ-component of the vorticity vector

$$\omega_\theta=\frac{\partial V_r}{\partial z}-\frac{\partial V_z}{\partial r}. \tag{4}$$

Equations (2a, b, c) lead through straightforward calculations to the following system in ψ_θ, V_θ, ω_θ:

$$-\frac{\partial}{\partial z}\left(\frac{1}{r}\frac{\partial(r\psi_\theta)}{\partial z}\right)-\frac{\partial}{\partial r}\left(\frac{1}{r}\frac{\partial(r\psi_\theta)}{\partial r}\right)=\omega_\theta, \tag{5a}$$

$$\frac{\partial(r V_\theta)}{\partial t}+V_r\frac{\partial(r V_\theta)}{\partial r}+V_z\frac{\partial(r V_\theta)}{\partial z}=0, \tag{5b}$$

$$\frac{\partial(\omega_\theta/r)}{\partial t}+V_r\frac{\partial(\omega_\theta/r)}{\partial r}+V_z\frac{\partial(\omega_\theta/r)}{\partial z}=\frac{1}{r^2}\frac{\partial(V_\theta^2)}{\partial z}. \tag{5c}$$

With the identities (3), the above system defines the flow completely. It is the basic model of this work.

Remark 2

Equation (5a) is a simple elliptic equation in $r\psi_\theta$. Equations (5b) and (5c) appear as transport equations of rV_θ and ω_θ/r respectively along the streamlines, with the presence of a left-hand term in (5c).

3. THE BOUNDARY CONDITIONS

Let Ω denote in the sequel a bounded open set of $\mathbb{R}^2$ with boundary Γ such that for every point of co-ordinates (z, r) in Ω we have

$$0<r_0 \leqslant r \leqslant r_1. \tag{6}$$

The classical inviscid boundary condition

$$\mathbf{u}\cdot\mathbf{n} = 0 \tag{7}$$

leads to the following condition on ψ_θ.

$$\operatorname{curl}(r\psi_\theta)\cdot\mathbf{n} = 0. \tag{8}$$

Thus we get

$$r\psi_\theta|_{\Gamma_i} = c_i, \tag{9}$$

where the c_i are constant, for each component Γ_i of the boundary Γ.

3.1. Model 1

As a theoretical model, we consider the case of a simply connected domain Ω with the boundary condition

$$r\psi_\theta|_\Gamma = 0. \tag{10}$$

3.2. Model 2

Now we turn to a more realistic case. Ω will denote the meridian section of an annular duct (Figure 1). Γ_0 and Γ_1 are assumed to be slipping walls. On the upstream boundary Γ_{in} the velocity field is given. On the downstream boundary Γ_{out} we assume only that the radial component of the velocity is zero.

This model represents the flow around an axisymmetric body. The boundary Γ_1 is assumed far enough from Γ_0 to be a horizontal stream surface, which leads to the following boundary conditions for ψ_θ, V_θ and ω_θ.

On Γ_{in}, Γ_0 and Γ_1 we deduce the values of ψ_θ, V_θ and ω_θ from the given velocity field. With $r\psi_\theta$ defined up to a constant, we are able to choose $r\psi_\theta = 0$ on Γ_0. Then the law of $r\psi_\theta$ on Γ_{in} is completely known and we get the constant value c of $r\psi_\theta$ on Γ_1.

On Γ_{out} the condition $V_r = 0$ leads to the homogenous Neumann boundary condition

$$\left.\frac{\partial(r\psi_\theta)}{\partial n}\right|_{\Gamma_{out}} = 0 \tag{11}$$

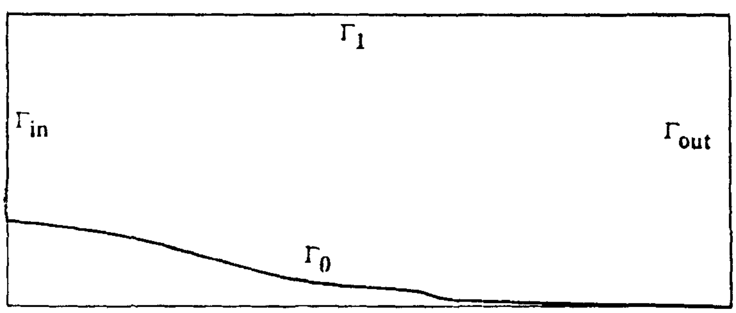

Figure 1. The axisymmetric duct

3.3. Model 3

Let us now consider the same annular duct but with an axisymmetric aerofoil-shaped body inside (Figure 2). On the aerofoil boundary Γ_2 we have the inviscid boundary condition

$$\mathbf{u}\cdot\mathbf{n}=0, \tag{12}$$

which leads to

$$r\psi_\theta|_{\Gamma_2}=c_2. \tag{13}$$

The problem is then to determine the physically correct value of the constant c_2. This has been done by using a Kutta–Joukovski condition. This condition implies the equality of the static pressures at the upper and lower sides of the trailing edge.

We made the computation in the following manner (F. Hecht, private communication). We looked for a streamfunction $r\psi_\theta$ given by

$$r\psi_\theta=\psi_0+\alpha\psi_1, \tag{14}$$

with ψ_0 the solution of equations (5a) at each time step, with the real boundary condition, except on Γ_2 where we take

$$\psi_0|_{\Gamma_2}=0, \tag{15}$$

and ψ_1 the solution of the simple homogeneous equation

$$-\frac{\partial}{\partial z}\left(\frac{1}{r}\frac{\partial\psi_1}{\partial z}\right)-\frac{\partial}{\partial r}\left(\frac{1}{r}\frac{\partial\psi_1}{\partial r}\right)=0, \tag{16}$$

with all the Dirichlet boundary conditions equal to zero except on Γ_2 where we take

$$\psi_1|_{\Gamma_2}=1. \tag{17}$$

The parameter α is then computed at each time step in order to satisfy the equality of the static pressures at the upper and lower sides of the trailing edge.

$$P_s^+=P_s^-; \tag{18}$$

i.e.

$$|\mathrm{curl}(\psi_0+\alpha\psi_1)|_+^2-|\mathrm{curl}(\psi_0+\alpha\psi_1)|_-^2=\frac{2}{\rho}(P^+-P^-), \tag{19}$$

where P^+ and P^- are the pressures on the upper and lower sides of the trailing edge (Figure 3).

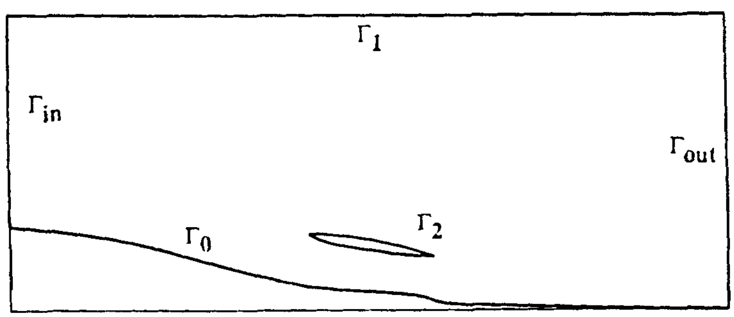

Figure 2. The complete model geometry

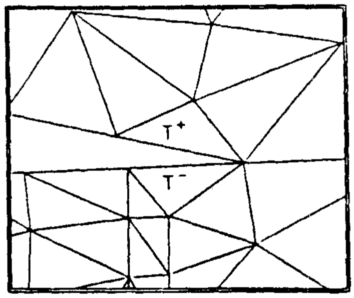

Figure 3. The numerical treatment of the Kutta–Joukovski condition

This quadratic equation in α has two solutions. The right one is the root for which the normal velocities are opposite.

4. FINITE ELEMENT APPROXIMATION

In order to derive a finite element approximation of the problem, we need to introduce a variational form of the axisymmetric Euler equations.

4.1. Basic concepts and function spaces

Let $(\,.\,,\,.\,)$ denote the axisymmetric scalar product in $L^2(\Omega)$,

$$(u, v) = \iint_\Omega uvr\,\mathrm{d}r\,\mathrm{d}z, \tag{20}$$

and $\|\cdot\|_{0,\Omega}$ the associated norm in $L^2(\Omega)$. For $m \in \mathbb{N}$ and $p \in \mathbb{R}$ with $1 \leqslant p \leqslant +\infty$ we define the Sobolev space

$$W^{m,p}(\Omega) = \{v \in L^p(\Omega); \partial^\alpha v \in L^p(\Omega), \forall |\alpha| \leqslant m\},$$

which is a Banach space for the norm

$$\|v\|_{m,p,\Omega} = \left(\sum_{|\alpha| \leq m} \iint_\Omega |\partial^\alpha v(x)|^p r\,\mathrm{d}r\,\mathrm{d}z\right)^{1/p}, \quad p < +\infty \tag{21}$$

or

$$\|v\|_{m,\infty,\Omega} = \sup_{|\alpha| \leqslant m} \left(\sup_{x \in \Omega} \mathrm{ess}\,|\partial^\alpha v(x)|\right), \quad p = +\infty. \tag{22}$$

we also provide $W^{m,p}(\Omega)$ with the following semi-norm:

$$|v|_{m,p,\Omega} = \left(\sum_{|\alpha| = m} \int_\Omega |\partial^\alpha v(x)|^p r\,\mathrm{d}r\,\mathrm{d}z\right)^{1/p} \quad \text{for } p < +\infty. \tag{23}$$

$$|v|_{m,\infty,\Omega} = \sup_{|\alpha| \leq m} \left(\sup_{x \in \Omega} \mathrm{ess}\,|\partial^\alpha v(x)|\right) \quad \text{for } p = +\infty. \tag{24}$$

In the special case $p = 2$ we obtain the Hilbert space $H^m(\Omega)$ with the norm $\|\cdot\|_{m,\Omega}$ and the semi-norm $|\cdot|_{m,\Omega}$.

Let us introduce the bilinear form on $(H^1(\Omega))^2$,

$$a:(u, v)\rightarrow a(u, v),$$

$$a(u, v)=\int\int_{\Omega}\frac{1}{r}\left(\frac{\partial u}{\partial r}\frac{\partial v}{\partial r}+\frac{\partial u}{\partial z}\frac{\partial v}{\partial z}\right)\mathrm{d}r\mathrm{d}z, \tag{25}$$

and the trilinear form on $W^{1,\infty}(\Omega)\times H^1(\Omega)\times L^2(\Omega)$,

$$b:(u, v, w)\rightarrow b(u, v, w),$$

$$b(u, v, w)=\int\int_{\Omega}\left(\frac{\partial u}{\partial z}\frac{\partial v}{dr}-\frac{\partial u}{\partial r}\frac{\partial v}{\partial z}\right)w\,\mathrm{d}r\mathrm{d}z. \tag{26}$$

4.2. Properties of the linear forms a and b

4.2.1. The linear form a. Since for every point (z, r) in Ω we assumed that

$$0<r_0\leq r\leq r_1,$$

the bilinear form a is, as in the two-dimensional case, continuous in $(H^1(\Omega))^2$ and $H_0^1(\Omega)$ – Elliptic. Moreover, we have the following inequalities:

$$\frac{\alpha}{r_1^2}||u||_{1,r}^2\leq\frac{1}{r_1^2}|u|_{1,\Omega}^2\leq a(u, u)\quad\forall u\in H_0^1(\Omega), \tag{27}$$

$$|a(u, v)|\leq\frac{1}{r_0^2}|u|_{1,\Omega}|v|_{1,\Omega}\quad\forall u, v\in H^1(\Omega). \tag{28}$$

4.2.2. The form b. The trilinear form b satisfies the following properties.

(1) b is continuous in $W^{1,\infty}(\Omega)\times H^1(\Omega)\times L^2(\Omega)$.

(2) $\forall u\in W_0^{1,\infty}(\Omega)$, $v\in H^1(\Omega)$ we have

$$b(u, v, v)=b(u, v, u)=0. \tag{29}$$

Proof. (1)

$$|b(u, v, w)|=\left|\int\int_{\Omega}\left(\frac{\partial u}{\partial z}\frac{\partial v}{\partial r}-\frac{\partial u}{\partial r}\frac{\partial v}{\partial z}\right)\frac{w}{r}\,r\mathrm{d}r\mathrm{d}z\right|,$$

so that

$$|b(u, v, w)|\leq\frac{1}{r_0}\left|\left|\frac{\partial u}{\partial z}\frac{\partial v}{\partial r}-\frac{\partial u}{\partial r}\frac{\partial v}{\partial z}\right|\right|_{0,\Omega}||w||_{0,\Omega}$$

and

$$|b(u, v, w)|\leq\frac{1}{r_0}|u|_{1,\infty,\Omega}||w||_{0,\Omega}. \tag{30}$$

(2) The form b is exactly the same as the form of the convective term in the two-dimensional Euler equations and we refer to reference 1 for the proof.

4.3. Variational formulation

Using a classical Green formula, we obtain, in the case of model 1, the following variational formulation of equations (5a, b, c). Find a function $t \in [0, T] \to (\psi_\theta(t), v_\theta(t), \omega_\theta(t)) \in H_0^1(\Omega) \times H^1(\Omega) \times H^1(\Omega)$ such that

$$\mathrm{E}\begin{cases} a(r\psi_\theta(t), u) = \left(\dfrac{\omega_\theta}{r}(t), u\right) \quad \forall u \in H_0^1(\Omega), & (31\mathrm{a}) \\ \left(\dfrac{\mathrm{d}}{\mathrm{d}t} r v_\theta(t), v\right) = b(r\psi_\theta(t), r v_\theta(t), v) \quad \forall v \in H^1(\Omega) & (31\mathrm{b}) \\ \left(\dfrac{\mathrm{d}}{\mathrm{d}t}\dfrac{\omega_\theta}{r}(t), w\right) = b\left(r\psi_\theta(t), \dfrac{\omega_\theta}{r}(t), w\right) + \left(\dfrac{1}{r^2}\dfrac{\partial}{\partial z}(v_\theta^2(t)), w\right) \quad \forall w \in H^1(\Omega). & (31\mathrm{c}) \end{cases}$$

4.4. Conservation properties of problem E

Using the fundamental property (29) of the trilinear form b we derive the following results:

(1)
$$\frac{1}{2}\frac{\mathrm{d}}{\mathrm{d}t} \| r v_\theta(t) \|_{0,\Omega}^2 = b(r\psi_\theta(t), r v_\theta(t), r v_\theta(t)) = 0 \quad \forall t \in [0, T]. \tag{32}$$

Thus we get the conservation of the L^2-norm of $r v_\theta(t)$:

$$\| r v_\theta(t) \|_{0,\Omega} = \| r v_\theta(0) \|_{0,\Omega} \quad \forall t \in [0, T]. \tag{33}$$

(2)
$$\frac{1}{2}\frac{\mathrm{d}}{\mathrm{d}t} \left\| \frac{\omega_\theta}{r}(t) \right\|_{0,\Omega}^2 = b\left(r\psi_\theta(t), \frac{\omega_\theta}{r}(t), \frac{\omega_\theta}{r}(t)\right) + \left(\frac{1}{r^2}\frac{\partial}{\partial z}(v_\theta^2(t)), \frac{\omega_\theta}{r}(t)\right), \tag{34}$$

so that

$$\frac{\mathrm{d}}{\mathrm{d}t} \left\| \frac{\omega_\theta}{r}(t) \right\|_{0,\Omega} \le \frac{1}{r_0^2} \left\| \frac{\partial}{\partial z}(v_\theta^2(t)) \right\|_{0,\Omega} \tag{35}$$

and finally

$$\left\| \frac{\omega_\theta}{r}(t) \right\|_{0,\Omega} \le \left\| \frac{\omega_\theta}{r}(0) \right\|_{0,\Omega} + \frac{1}{r_0^2} \int_0^t \left\| \frac{\partial}{\partial z}(v_\theta^2(t)) \right\|_{0,\Omega} \mathrm{d}t. \tag{36}$$

Remark

In the particular case of an initial value of v_θ equal to zero, v_θ remains null for all $t \in [0, T]$ and the system E reduces to two coupled equations involving $r\psi_\theta$ and ω_θ / r. Moreover, in that case we get

$$\left\| \frac{\omega_\theta}{r}(t) \right\|_{0,\Omega} = \left\| \frac{\omega_\theta}{r}(0) \right\|_{0,\Omega} \quad \forall t \in [0, T]. \tag{37}$$

4.5. Generalization

4.5.1. In the case of model 2 the test function space in the first elliptic equation (31a) is replaced by the space V defined by

$$V = \{ v \in H^1(\Omega);\, v = 0 \quad \text{on} \quad \Gamma_{\mathrm{in}} \cup \Gamma_0 \cup \Gamma_1 \}$$

The unknown streamfunction $r\psi_\theta$ satisfies the following boundary conditions: $r\psi_\theta$ given on Γ_{in}; $r\psi_\theta = 0$ on Γ_0 and $r\psi_\theta = c$ (given constant) on Γ_1; $\partial(r\psi_\theta)/\partial n = 0$ on Γ_{out}.

4.5.2. In the case of model 3 we also have to take into account a Kutta–Joukovski condition (see Section 3.3). We made the computations as follows.

The stream function ψ_1 has been computed once and for all at the beginning of the program. It does not depend on time. Then we just have to solve one elliptic equation at each time step to get the complete streamfunction (Figure 4).

4.6. Finite element spatial approximation

Let U_h and V_h be two finite dimensional spaces such that $U_h \subset W_0^{1,\infty}(\Omega)$ and $V_h \subset W^{1,\infty}(\Omega)$. We approximate the continuous problem (E) by the following approximate problem (E_h). Find a function $t \in [0, T] \to (\psi_{\theta,h}(t), v_{\theta,h}(t), \omega_{\theta,h}(t)) \in U_h \times V_h \times V_h$ satisfying for all $t \in [0, T]$

$$
E_h \begin{cases} a(r\psi_{\theta,h}(t), u_h) = \left(\dfrac{\omega_{\theta,h}}{r}(t), u_h\right) \quad \forall u_h \in U_h, & (38a) \\ \left(\dfrac{d}{dt} rv_{\theta,h}(t), v_h\right) = b(r\psi_{\theta,h}(t), rv_{\theta,h}(t), v_h) \quad \forall v_h \in V_h, & (38b) \\ \left(\dfrac{d}{dt}\dfrac{\omega_{\theta,h}}{r}(t), w_h\right) = b\left(r\psi_{\theta,h}(t), \dfrac{\omega_{\theta,h}}{r}(t), w_h\right) + \left(\dfrac{1}{r^2}\dfrac{\partial}{\partial z}(v_{\theta,h}^2(t)), w_h\right) \quad \forall w_h \in V_h. & (38c) \end{cases}
$$

4.6.1. Conservation properties of problem E_h. We get for the approximate solution $r\psi_{\theta,h}$, $rv_{\theta,h}$ and $\omega_{\theta,h}/r$ the same bounds as for the exact solution. For instance,

$$\|rv_{\theta,h}(t)\|_{0,\Omega} = \|rv_{\theta,h}(0)\|_{0,\Omega} \quad \forall t \in [0, T].$$

4.6.2. A first convergence result. Let us consider the simplest model problem E^* in the particular case of $V_\theta = 0$ (flow without 'swirl'). The corresponding approximate problem E_h^* reduces to the following system of two equations in ψ_θ and ω_θ:

$$
E_h^* \begin{cases} a(r\psi_{\theta,h}(t), u_h) = \left(\dfrac{\omega_{\theta,h}}{r}(t), u_h\right) \quad \forall u_h \in U_h, & (39a) \\ \left(\dfrac{d}{dt}\dfrac{\omega_{\theta,h}}{r}(t), v_h\right) = b\left(r\psi_{\theta,h}(t), \dfrac{\omega_{\theta,h}}{r}(t), v_h\right) \quad \forall v_h \in V_h. & (39b) \end{cases}
$$

Assume that the $(\psi_\theta, \omega_\theta)$ solution of the problem E^* belongs to the space

$$L^\infty(0, T; [W^{k+1,\infty}(\Omega) \cup W_0^{1,\infty}(\Omega)] \times W^{k+1,\infty}(\Omega))$$

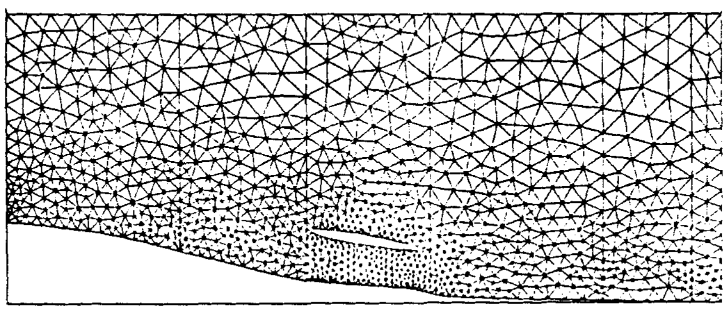

Figure 4. The computational mesh in the case of the complete model

Then under classical hypotheses of finite element interpolation we get the following error bound:

$$|\psi_\theta(t)-\psi_{\theta,h}(t)|_{1,\Omega}+\|\omega_\theta(t)-\omega_{\theta,h}(t)\|_{0,\Omega}\leq Ch^k \tag{40}$$

Proof: The proof follows the same lines as the proof of the convergence of the finite element method in the two-dimensional case.[1] In fact the form b here is exactly the same as in the two-dimensional case and there are just slight differences in the expressions of the bilinear form a and the scalar product. These differences are very easy to handle since we can assume that hypotheses (6) hold.

Remark: *the general case*

The general case is more tricky because of the term

$$\left(\frac{1}{r^2}\frac{\partial}{\partial z}(v_{\theta,h}^2(t)),\ w_h\right)$$

in equation (38c). We have not yet succeeded in proving the convergence of the finite element scheme in this case.

5. TIME DISCRETIZATION

Let us choose a positive integer N, let Δt denote the corresponding time step,

$$\Delta t=T/N,$$

and (t_n) the subdivision of $[0,\ T]$,

$$t_n=n\,\Delta t \quad \text{for} \quad 0\leq n\leq N.$$

Let $\psi_{\theta,h}^n$, $v_{\theta,h}^n$ and $\omega_{\theta,h}^n$ denote approximations of $\psi_\theta(t_n)$, $v_\theta(t_n)$ and $\omega_\theta(t_n)$ respectively.

5.1. *The leap-frog scheme*

The leap-frog scheme for the problem E can be written as

$$a(r\psi_{\theta,h}^n,u_h)=\left(\frac{\omega_{\theta,h}^n}{r},u_h\right)\quad \forall u_h\in U_h, \tag{41a}$$

$$(rv_{\theta,h}^{n+1}-rv_{\theta,h}^{n-1},v_h)=2\Delta t\ b(r\psi_{\theta,h}^n,rv_{\theta,h}^n,v_h)\quad \forall v_h\in V_h, \tag{41b}$$

$$\left(\frac{\omega_{\theta,h}^{n+1}}{r}-\frac{\omega_{\theta,h}^{n-1}}{r},w_h\right)=2\Delta t\left[b\left(r\psi_{\theta,h}^n,\frac{\omega_{\theta,h}^n}{r},w_h\right)+\left(\frac{1}{r^2}\frac{\partial}{\partial z}(v_{\theta,h}^n)^2,w_h\right)\right]\quad \forall w_h\in V_h, \tag{41c}$$

with $\psi_{\theta,h}^0$, $v_{\theta,h}^0$ and $\omega_{\theta,h}^0$ given and $\psi_{\theta,h}^1$, $v_{\theta,h}^1$ and $\omega_{\theta,h}^1$ solutions of

$$a(r\psi_{\theta,h}^1,u_h)=\left(\frac{\omega_{\theta,h}^1}{r},u_h\right)\quad \forall u_h\in U_h, \tag{41d}$$

$$(rv_{\theta,h}^1-rv_{\theta,h}^0,v_h)=\Delta t\,b(r\psi_{\theta,h}^0,rv_{\theta,h}^0,v_h)\quad \forall v_h\in V_h, \tag{41e}$$

$$\left(\frac{\omega_{\theta,h}^1}{r}-\frac{\omega_{\theta,h}^0}{r},w_h\right)=\Delta t\left[b\left(r\psi_{\theta,h}^0,\frac{\omega_{\theta,h}^0}{r},w_h\right)+\left(\frac{1}{r^2}\frac{\partial}{\partial z}(v_{\theta,h}^0)^2,w_h\right)\right]\quad \forall w_h\in V_h. \tag{41f}$$

The stability of leap-frog scheme follows from the next lemma.

5.1.1. Lemma. Under the stability hypotheses

(1)
$$c\Delta t\left(\frac{1}{h}|r\psi^n_{\theta,h}|_{1,\infty,\Omega}+\frac{1}{r^4}|rv^n_{\theta,h}|_{1,\infty,\Omega}\right)<1 \quad \forall n\in 0, N, \tag{42}$$

(2) there exists a constant $A>0$ such that

$$\frac{C}{h}|r\psi^n_{\theta,h}-r\psi^{n-1}_{\theta,h}|_{1,\infty,\Omega}+\frac{c}{r^4}(|rv^n_{\theta,h}|_{1,\infty,\Omega}+|rv^{n+1}_{\theta,h}|_{1,\infty,\Omega})<A, \tag{43}$$

we have the following bound for every $n=0,\cdots,N$:

$$||rv^n_{\theta,h}||^2_{0,\Omega}+\left|\left|\frac{\omega^n_{\theta,h}}{r}\right|\right|^2_{0,\Omega}\leq C\left(||rv^0_{\theta,h}||^2_{0,\Omega}+||rv^1_{\theta,h}||^2_{0,\Omega}+\left|\left|\frac{\omega^0_{\theta,h}}{r}\right|\right|^2_{0,\Omega}+\left|\left|\frac{\omega^1_{\theta,h}}{r}\right|\right|^2_{0,\Omega}\right). \tag{44}$$

Proof: Let us introduce

$$\begin{aligned}S_n=||rv^n_{\theta,h}||^2_{0,\Omega}+||rv^{n+1}_{\theta,h}||^2_{0,\Omega}+\left|\left|\frac{w^n_{\theta,h}}{r}\right|\right|^2_{0,\Omega}+\left|\left|\frac{w^{n+1}_{\theta,h}}{r}\right|\right|^2_{0,\Omega}-2\Delta t\, b(r\psi^n_{\theta,h},rv^n_{\theta,h},rv^{n+1}_{\theta,h})\\ -2\Delta t\, b\left(r\psi^n_{\theta,h},\frac{\omega^n_{\theta,h}}{r},\frac{\omega^{n+1}_{\theta,h}}{r}\right)-2\Delta t\left(\frac{1}{r^2}\frac{\partial}{\partial z}(v^n_{\theta,h})^2,\frac{\omega^{n+1}_{\theta,h}}{r}\right).\end{aligned}$$

We follow, as in Reference 1, the energy method used by Richtmyer and Morton.
We have

$$|b(r\psi^n_{\theta,h},rv^n_{\theta,h},rv^{n+1}_{\theta,h})|\leq C|r\psi^n_{\theta,h}|_{1,\infty,\Omega}|rv^n_{\theta,h}|_{1,\Omega}||rv^{n+1}_{\theta,h}||_{0,\Omega},$$

and by use of the inverse inequality,

$$|b(r\psi^n_{\theta,h},rv^n_{\theta,h},rv^{n+1}_{\theta,h})|\leq\frac{C}{h}|r\psi^n_{\theta,h}|_{1,\infty,\Omega}||rv^n_{\theta,h}||_{0,\Omega}||rv^{n+1}_{\theta,h}||_{0,\Omega}.$$

Similarly we get

$$\left|b\left(r\psi^n_{\theta,h},\frac{\omega^n_{\theta,h}}{r},\frac{\omega^{n+1}_{\theta,h}}{r}\right)\right|\leq\frac{C}{h}|r\psi^n_{\theta,h}|_{1,\infty,\Omega}\left|\left|\frac{\omega^n_{\theta,h}}{r}\right|\right|_{0,\Omega}\left|\left|\frac{\omega^{n+1}_{\theta,h}}{r}\right|\right|_{0,\Omega}$$

and

$$\left|\left(\frac{1}{r^2}\frac{\partial}{\partial z}(v^n_{\theta,h})^2,\frac{\omega^{n+1}_{\theta,h}}{r}\right)\right|\leq\frac{c}{r_0^4}|rv^n_{\theta,h}|_{1,\infty,\Omega}||rv^n_{\theta,h}||_{0,\Omega}\left|\left|\frac{\omega^{n+1}_{\theta,h}}{r}\right|\right|_{0,\Omega},$$

so that

$$\begin{aligned}\left(1-C\frac{\Delta t}{h}|r\psi^n_{\theta,h}|_{1,\infty,\Omega}-c\frac{\Delta t}{r^4}|rv^n_{\theta,h}|_{1,\infty,\Omega}\right)\Bigg(||rv^n_{\theta,h}||^2_{0,\Omega}+||rv^{n+1}_{\theta,h}||^2_{0,\Omega}\\ +\left|\left|\frac{\omega^n_{\theta,h}}{r}\right|\right|^2_{0,\Omega}+\left|\left|\frac{\omega^{n+1}_{\theta,h}}{r}\right|\right|^2_{0,\Omega}\Bigg)\leq S_n\leq\left(1+C\frac{\Delta t}{h}|r\psi^n_{\theta,h}|_{1,\infty,\Omega}+c\frac{\Delta t}{r^4}|rv^n_{\theta,h}|_{1,\infty,\Omega}\right)\\ \times\left(||rv^n_{\theta,h}||^2_{0,\Omega}+||rv^{n+1}_{\theta,h}||^2_{0,\Omega}+\left|\left|\frac{\omega^n_{\theta,h}}{r}\right|\right|^2_{0,\Omega}+\left|\left|\frac{\omega^{n+1}_{\theta,h}}{r}\right|\right|^2_{0,\Omega}\right).\end{aligned}$$

But we also have

$$S_n - S_{n-1} = ||rv_{\theta,h}^{n+1}||_{0,\Omega}^2 - ||rv_{\theta,h}^{n-1}||_{0,\Omega}^2 + \left|\left|\frac{\omega_{\theta,h}^{n+1}}{r}\right|\right|_{0,\Omega}^2 - \left|\left|\frac{\omega_{\theta,h}^{n-1}}{r}\right|\right|_{0,\Omega}^2$$

$$- 2\Delta t\, b(r\psi_{\theta,h}^n, rv_{\theta,h}^n, rv_{\theta,h}^{n+1}) + 2\Delta t\, b(r\psi_{\theta,h}^{n-1}, rv_{\theta,h}^{n-1}, rv_{\theta,h}^n)$$

$$- 2\Delta t\, b\left(r\psi_{\theta,h}^n, \frac{\omega_{\theta,h}^n}{r}, \frac{\omega_{\theta,h}^{n+1}}{r}\right) + 2\Delta t\, b\left(r\psi_{\theta,h}^{n-1}, \frac{\omega_{\theta,h}^{n-1}}{r}, \frac{\omega_{\theta,h}^n}{r}\right)$$

$$- 2\Delta t\left(\frac{1}{r^2}\frac{\partial}{\partial z}(v_{\theta,h}^n)^2, \frac{\omega_{\theta,h}^{n+1}}{r}\right) + 2\Delta t\left(\frac{1}{r^2}\frac{\partial}{\partial z}(v_{\theta,h}^{n-1})^2, \frac{\omega_{\theta,h}^n}{r}\right)$$

Using then

$$||rv_{\theta,h}^{n+1}||_{0,\Omega}^2 - ||rv_{\theta,h}^{n-1}||_{0,\Omega}^2 = 2\Delta t\, b(r\psi_{\theta,h}^n, rv_{\theta,h}^n, rv_{\theta,h}^{n-1} + rv_{\theta,h}^{n+1})$$

and

$$\left|\left|\frac{\omega_{\theta,h}^{n+1}}{r}\right|\right|_{0,\Omega}^2 - \left|\left|\frac{\omega_{\theta,h}^{n-1}}{r}\right|\right|_{0,\Omega}^2 = 2\Delta t\left[b\left(r\psi_{\theta,h}^n, \frac{\omega_{\theta,h}^n}{r}, \frac{\omega_{\theta,h}^{n-1}}{r} + \frac{\omega_{\theta,h}^{n+1}}{r}\right)\right.$$

$$\left. + \left(\frac{1}{r^2}\frac{\partial}{\partial z}(v_{\theta,h}^n)^2, \frac{\omega_{\theta,h}^{n-1}}{r} + \frac{\omega_{\theta,h}^{n+1}}{r}\right)\right],$$

we get

$$S_n - S_{n-1} = 2\Delta t\left[b(r\psi_{\theta,h}^n - r\psi_{\theta,h}^{n-1}, rv_{\theta,h}^n, rv_{\theta,h}^{n-1}) + b\left(r\psi_{\theta,h}^n - r\psi_{\theta,h}^{n-1}, \frac{\omega_{\theta,h}^n}{r}, \frac{\omega_{\theta,h}^{n-1}}{r}\right)\right.$$

$$\left. + \left(\frac{1}{r^2}\frac{\partial}{\partial z}(v_{\theta,h}^n)^2, \frac{\omega_{\theta,h}^{n-1}}{r}\right) + \left(\frac{1}{r^2}\frac{\partial}{\partial z}(v_{\theta,h}^{n-1})^2, \frac{\omega_{\theta,h}^n}{r}\right)\right].$$

Thus we get

$$S_n - S_{n-1} \leq \frac{2c\Delta t}{h}\left[|r\psi_{\theta,h}^n - r\psi_{\theta,h}^{n-1}|_{1,\infty,\Omega}\left(||rv_{\theta,h}^n||_{0,\Omega}||rv_{\theta,h}^{n-1}||_{0,\Omega} + \left|\left|\frac{\omega_{\theta,h}^n}{r}\right|\right|_{0,\Omega}\left|\left|\frac{\omega_{\theta,h}^{n-1}}{r}\right|\right|_{0,\Omega}\right)\right]$$

$$+ \frac{2c\Delta t}{r_0^4}\left(|rv_{\theta,h}^n|_{1,\infty,\Omega}||rv_{\theta,h}^n||_{0,\Omega}\left|\left|\frac{\omega_{\theta,h}^{n-1}}{r}\right|\right|_{0,\Omega} + |rv_{\theta,h}^{n-1}|_{1,\infty,\Omega}||rv_{\theta,h}^{n-1}||_{0,\Omega}\left|\left|\frac{\omega_{\theta,h}^n}{r}\right|\right|_{0,\Omega}\right),$$

$$S_n - S_{n-1} \leq \left(\frac{c\Delta t}{h}|r\psi_{\theta,h}^n - r\psi_{\theta,h}^{n-1}|_{1,\infty,\Omega} + \frac{c\Delta t}{r^4}(|rv_{\theta,h}^n|_{1,\infty,\Omega} + |rv_{\theta,h}^{n-1}|_{1,\infty,\Omega})\right)$$

$$\times\left(||rv_{\theta,h}^n|_{0,\Omega}^2 + ||rv_{\theta,h}^{n-1}||_{0,\Omega}^2 + \left|\left|\frac{\omega_{\theta,h}^n}{r}\right|\right|_{0,\Omega}^2 + \left|\left|\frac{\omega_{\theta,h}^{n-1}}{r}\right|\right|_{0,\Omega}^2\right),$$

and by use of the stability hypotheses we derive

$$||rv_{\theta,h}^n||_{0,\Omega}^2 + ||rv_{\theta,h}^{n-1}||_{0,\Omega}^2 + \left|\left|\frac{\omega_{\theta,h}^n}{r}\right|\right|_{0,\Omega}^2 + \left|\left|\frac{\omega_{\theta,h}^{n-1}}{r}\right|\right|_{0,\Omega}^2 \leq KS_0$$

$$+ AK\,\Delta t\sum_{m=1}^{n}\left(||rv_{\theta,h}^m||_{0,\Omega}^2 + ||rv_{\theta,h}^{m-1}||_{0,\Omega}^2 + \left|\left|\frac{\omega_{\theta,h}^m}{r}\right|\right|_{0,\Omega}^2 + \left|\left|\frac{\omega_{\theta,h}^{m-1}}{r}\right|\right|_{0,\Omega}^2\right)$$

and the result.

5.2. A semi-implicit scheme of order two

This scheme is a semi-implicit Crank–Nicolson scheme. It can be written as follows in a finite element context:

$$a(r\psi^n_{\theta,h}, u_h)=\left(\frac{\omega^n_{\theta,h}}{r}, u_h\right) \quad \forall u_h \in U_h, \tag{45a}$$

$$a(r\psi^{(n+\frac{1}{2})}_{\theta,h}, u_h)=\left(\frac{\omega^n_{\theta,h}}{r}, u_h\right)+\frac{\Delta t}{2}\left[b\left(r\psi^n_{\theta,h}, \frac{\omega^n_{\theta,h}}{r}, u_h\right)+\left(\frac{1}{r^2}\frac{\partial}{\partial z}(v^n_{\theta,h})^2, u_h\right)\right] \quad \forall u_h \in U_h, \tag{45b}$$

$$(rv^{n+1}_{\theta,h}-rv^n_{\theta,h}, v_h)=\frac{\Delta t}{2}b(r\psi^{(n+\frac{1}{2})}_{\theta,h}, rv^n_{\theta,h}+rv^{n+1}_{\theta,h}, v_h) \quad \forall v_h \in V_h, \tag{45c}$$

$$\left(\frac{\omega^{n+1}_{\theta,h}}{r}-\frac{\omega^n_{\theta,h}}{r}, w_h\right)=\frac{\Delta t}{2}\left[b\left(r\psi^{(n+\frac{1}{2})}_{\theta,h}, \frac{\omega^n_{\theta,h}}{r}+\frac{\omega^{n+1}_{\theta,h}}{r}, w_h\right)\right.$$
$$\left.+\left(\frac{1}{r^2}\left(\frac{\partial}{\partial z}(v^n_{\theta,h})^2+\frac{\partial}{\partial z}(v^{n+1}_{\theta,h})^2\right), w_h\right)\right] \quad \forall w_h \in V_h. \tag{45d}$$

This scheme is of order two in time and satisfies the following stability property. Let us assume that there exists a constant A such that we get the inequality

$$\left\|\frac{1}{r^2}\frac{\partial}{\partial z}(v^n_{\theta,h})^2+\frac{1}{r^2}\frac{\partial}{\partial z}(v^{n+1}_{\theta,h})^2\right\|_{0,\Omega}\leq A. \tag{46}$$

The preceding scheme is stable and we easily get

$$\|rv^n_{\theta,h}\|_{0,\Omega}=\|rv^0_{\theta,h}\|_{0,h} \quad \forall n=0,1,\cdots,N, \tag{47}$$

$$\left\|\frac{\omega^n_{\theta,h}}{r}\right\|_{0,\Omega}\leq\left\|\frac{\omega^0_{\theta,h}}{r}\right\|_{0,\Omega}+\frac{AT}{2}. \tag{48}$$

5.3. Methods of characteristics

For the application of the method of characteristics to the transport equations (5b) and (5c) in a finite element context we refer to Reference 6.

5.4 Numerical tests

The numerical tests have shown that the explicit leap-frog (Figure 5) scheme requires very small time steps in order to satisfy the stability condition. The semi-implicit scheme is better (Figure 6). Although it is more costly for each time step, it can work with much larger Δt and is globally faster.

However, the best results for the time-dependent transport equation were obtained by the use of the characteristics method. See Reference 6 for a comparison of these schemes.

6. AN ITERATIVE METHOD FOR THE STATIONARY SOLUTION

In order to get the stationary solution of the Euler equations (5a, b, c) we can of course use the time discretization schemes quoted above. However, it is a better choice with respect to numerical stability and computational time to use the following simple version of the characteristics method. This implementation essentially uses our ready knowledge of the streamlines, which is the case for plane or axisymmetric flow problems.

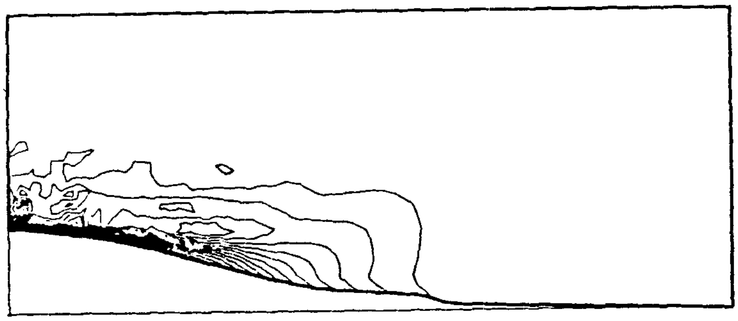

Figure 5. The vorticity (ω_θ/r) field at $t=1$ computed by the leap-frog scheme with $\Delta t=0{\cdot}001$

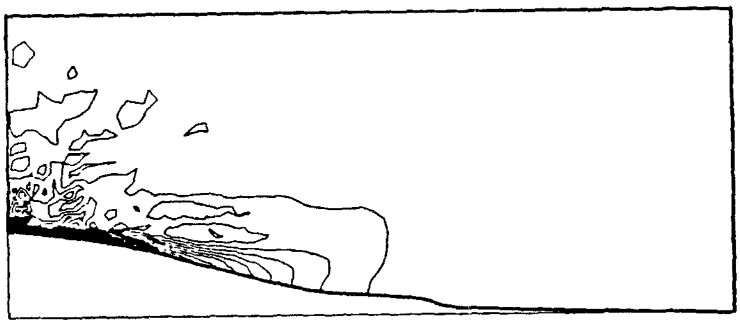

Figure 6. The vorticity (ω_θ/r) field at $t=1$ computed by the semi-implicit scheme with $\Delta t=0{\cdot}01$

Let us consider the simplest model without swirl (i.e. with $V_\theta=0$) to explain the method. In this case the problem reduces to the problem E*, the vortex ω_θ/r being simply convected along the streamlines $r\psi_\theta=$constant.

Thus to determine ω_θ/r at any point x of the domain Ω we just have to find on which streamlines the point x lies. Then we go back along this streamline to the entry point on the upstream boundary where the value of the vortex is given. We can summarize the computational process by the following iteration method.

Suppose that $\psi^0_{\theta,h}$ is given at time t_0. Then for any $n\geq 0$ define $\psi^{n+1}_{\theta,h}$ for $\psi^n_{\theta,h}$ by

$$a(r\psi^{n+1}_{\theta,h},u_h)=\left(\frac{\omega^n_{\theta,h}}{r},u_h\right)=(\omega_i(\psi^n_{\theta,h}),u_h)\quad\forall u_h\in U_h, \tag{49}$$

where ω_i is the numerical function, defined from the given upstream boundary values of the flow, that gives the functional law between the values of $r\psi_\theta$ and those of ω_θ/r.

More generally we can consider the family of algorithms:

$\psi^0_{\theta,h}$ given at t_0;

then $\psi^{n+1}_{\theta,h}$ is computed from $\psi^n_{\theta,h}$ by

$$a(r\psi^{n+1}_{\theta,h},u_h)=a(r\psi^n_{\theta,h},u_h)-\rho(a(r\psi^n_{\theta,h},u_h)-(\omega_i(r\psi^n_{\theta,h}),u_h))\quad\forall u_h\in U_h. \tag{50}$$

If $\rho=1$ we recover (49).

Moreover, if ω_i is differentiable, we should be able to solve the problem by a Newton method such as the following:

$\psi^0_{\theta,h}$ given at t_0;

$$a(r\psi^{n+1}_{\theta,h}, u_h)-(\omega_i'(r\psi^n_{\theta,h})r\psi^{n+1}_{\theta,h}, u_h)=(\omega_i(r\psi^n_{\theta,h}), u_h)-(\omega_i'(r\psi^n_{\theta,h})r\psi^n_{\theta,h}, u_h) \quad \forall u_h\in U_h. \tag{51}$$

This kind of iteration has been studied by many authors. One can find an interesting discussion in Reference 10. See also Reference 11.

First of all we have the following theoretical result.[12]

Let us consider the following non-linear problem: find $u\in U$ such that

$$a(u,v)=(\omega(u),v) \quad \forall v\in U, \tag{52}$$

where a is a bilinear, continuous and strongly elliptic form which satisfies

$$\alpha||u||^2\le a(u,u) \quad \forall u\in U, \quad \text{with} \quad \alpha>0, \tag{53}$$

$$|a(u,v)|\le M||u||v|| \quad \forall u,v\in U, \tag{54}$$

and ω is a non-linear operator in U. Let us define A: $U\to U$ by

$$(A(u), v)=a(u,v)-(\omega(u),v) \quad \forall u,v\in U. \tag{55}$$

We have the following result.

Theorem

Suppose A is Lipschitz continuous on the bounded sets of U and suppose that A is strongly elliptic, i.e. there exists a constant $k>0$ such that

$$(A(u_2)-A(u_1),u_2-u_1)\ge k||u_2-u_1||^2 \quad \forall u_1,u_2\in U. \tag{56}$$

Then the problem (52) has a unique solution. Moreover, the iteration

u^0 given;
u^{n+1} defined from u^n by

$$a(u^{n+1},v)=a(u^n,v)-\rho(a(u^n,v)-(\omega(u^n),v)) \quad \forall v\in U \tag{57}$$

converges to the solution u of (52) for every constant ρ satisfying

$$0<\rho<\rho_M, \tag{58}$$

ρ_M being a positive constant depending on u^0 in general.

Let us make some comments on the ellipticity condition (56). In our case it implies that there exists a positive number k such that for all u_1 and u_2 in U we have

$$a(u_2-u_1,u_2-u_1)-(\omega_i(u_2)-\omega_i(u_1), u_2-u_1)\ge k||u_2-u_1||^2. \tag{59}$$

But a is strongly elliptic, with

$$a(u_2-u_1,u_2-u_1)\ge\alpha||u_2-u_1||^2. \tag{60}$$

Then the inequality will be obtained if we can ensure that

$$(\omega_i(u_2)-\omega_i(u_1),u_2-u_1)\le 0 \quad \forall u_1,u_2\in U, \tag{61}$$

or if we can suppose that ω_i satisfies a Lipschitz condition

$$\|\omega_i(u_2)-\omega_i(u_1)\|\leq L\|u_2-u_1\|, \tag{62}$$

with a Lipschitz constant L such that $L<\alpha$.

We remark that in this last case it is easy to prove the convergence of the iterations (49) by a contraction argument.

We do not know whether condition (59) is a necessary condition for the existence or the stability of the flow. We refer to Reference 13 for further considerations on the stability of stationary solutions of the Euler equations. Let us however point out the problem given in Figure 7.

In the case of a flow with a given velocity profile such that ω_i' is not bounded, we do have instability of the flow, and this is one of the main difficulties in modelling a propeller.

7. FIXED-POINT ITERATION ALGORITHM VERSUS TIME-DEPENDENT APPROACH

Let us denote by $\psi_{\theta,h}$ the stationary solution of the approximate problem E_h. When the fixed-point algorithm is convergent we get the following error bound for every iteration $n=0, \ldots, N$:

$$\|\psi_{\theta,h}^n-\psi_{\theta,h}\|_{1,\Omega}\leq Ck^n\|\psi_{\theta,h}^0-\psi_{\theta,h}\|, \tag{63}$$

with $k\leq 1$. The convergence rate depends on the value of k, but we shall get for sufficiently large n

$$\|\psi_{\theta,h}^n-\psi_{\theta,h}\|_{1,\Omega}\leq\varepsilon, \tag{64}$$

whatever ε may be. Then the global error is only a finite element interpolation error.

In contrast, in a time-dependent approach each iteration corresponds to a time step. We solve a differential equation of the type

$$\frac{\mathrm{d}}{\mathrm{d}t}\psi_{\theta,h}=T(\psi_{\theta,h}). \tag{65}$$

The best error bound we can get, by use of the Gronwall lemma, is the following:

$$\|\psi_{\theta,h}^n-\psi_{\theta,h}(t_n)\|_{1,\Omega}\leq C\exp(At_n)(\|\psi_{\theta,h}^0-\psi_{\theta,h}(0)\|+h^k). \tag{66}$$

Let us then suppose that the stationary solution is obtained at the time $T=t_N$. We then have the following inequality:

$$\|\psi_{\theta,h}^N-\psi_{\theta,h}\|_{1,\Omega}\leq C\exp(AT)(\|\psi_{\theta,h}^0-\psi_{\theta,h}(0)\|+h^k). \tag{67}$$

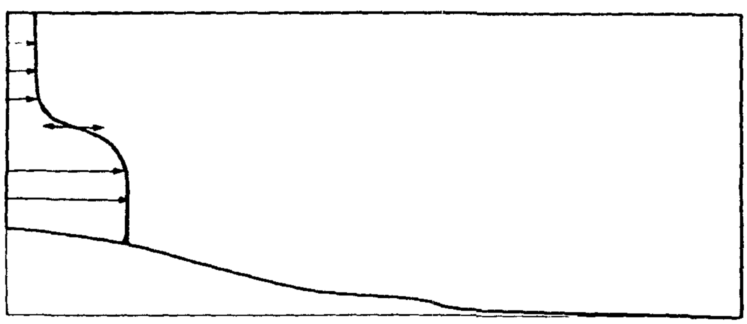

Figure 7.

The initial error and the interpolation error are multiplied by a factor $\exp(AT)$ which grows quickly with T. This is heuristic reason why the fixed-point iteration algorithm gives much better results than a time-dependent approach when one is only interested in the stationary solution (Figures 8 and 9).

8. MODELLING OF A DUCT PROPELLER

In order to model the presence of stators and rotors, we introduce jumps of the angular velocity V_θ and, for the rotors only, a jump of the pressure.

Let us say a few words about the computation of the pressure in our model. Pressures are convected along the streamlines from the upstream boundary to the downstream boundary. Then, when a streamline goes across a rotor, we add a jump of pressure in order to model the propeller effect. This increases the velocity in the duct through the Kutta–Joukovski condition. We also need, in that case, to introduce some viscosity effects at the trailing edge of the duct. After many numerical experiments and computational works, we determined two practical solutions.

First we introduce some amount of vorticity at the trailing edge in order to maintain the jump of axial velocity up and down to the trailing edge of the duct. The physically correct value for that jump was chosen as follows:

$$[\omega_\theta] = \frac{1}{\rho V_z}\frac{\partial P}{\partial r}. \tag{68}$$

This solution gives good results but may lead to computational instabilities.

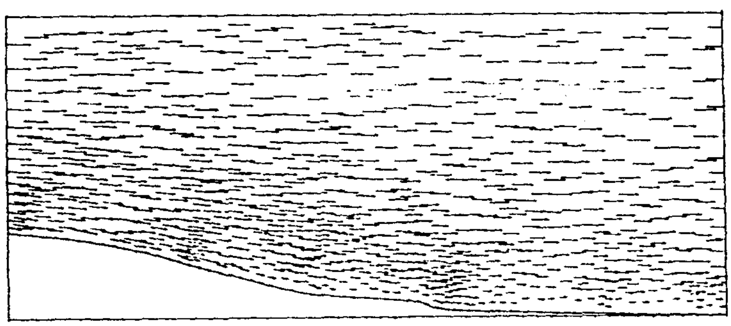

Figure 8. The velocity field of the stationary solution computed by our iterative method

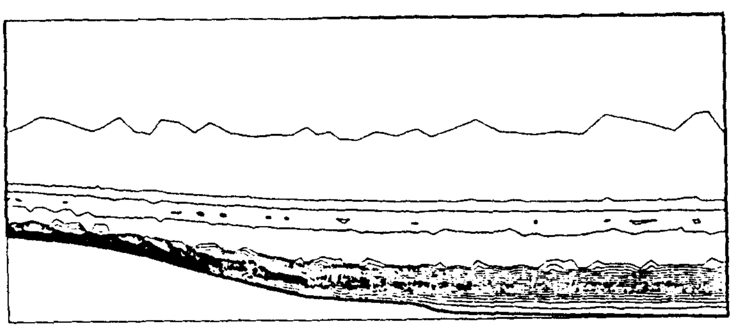

Figure 9. The vorticity (ω_θ/r) field of the stationary solution computed by our iterative method

The second solution prevents instabilities. We first make a computation to determine the geometry of the streamline passing by the trailing edge point. Then we completely compute the flow with this imposed streamline. Both methods have been compared and give similar results (Figures 10–12).

More detailed discussions, complete tests and a comparison with real experiments made at the Bassin des Carenes in Paris by B. Goirand are to appear (Figure 13).

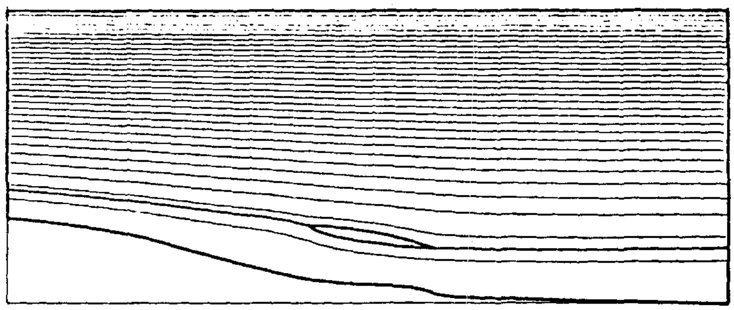

Figure 10. The streamlines of the stationary solution computed by our iterative method in the case of a duct propeller

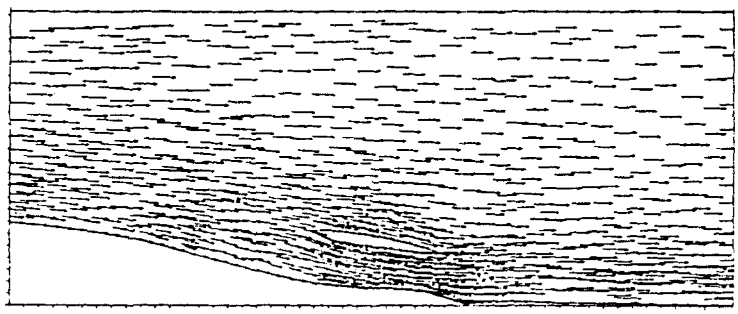

Figure 11. The velocity field of the stationary solution computed by our iterative method in the case of a duct propeller

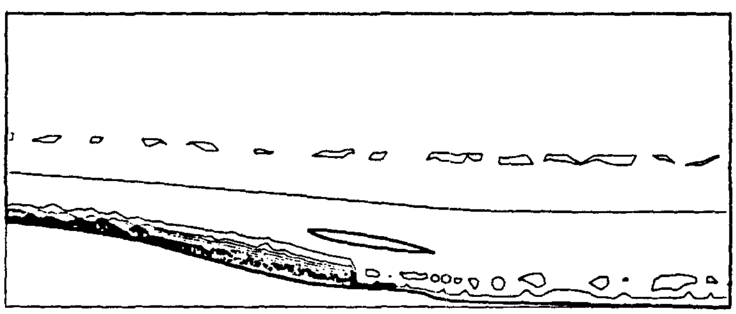

Figure 12. The vorticity (ω_θ/r) field of the stationary solution computed by our iterative method in the case of a duct propeller

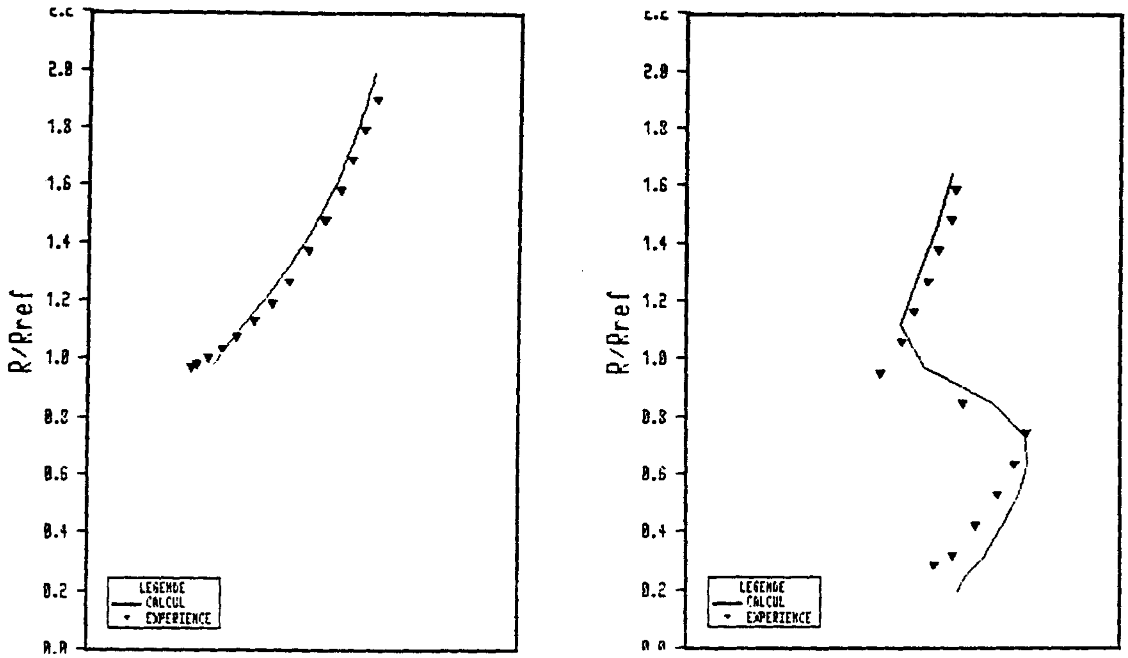

Figure 13. Comparison between computed and experimental velocity profiles before and after the propeller made by B. Goirand at the Bassin des Carenes in Paris

9. CONCLUSIONS

In this paper we presented a stable, precise and very fast solver, based on the characteristics method, for the stationary axisymmetric Euler equations. Its stability and computing time performance are well adapted to 'trial and error' procedures in engineering design. This scheme has been successfully used to compute an internal–external axisymmetric flow and to determine the whole propulsive performance, especially duct thrust and interaction between propulsor and stern. Comparisons with experiments made at the Bassin des Carenes in Paris have shown very good agreement between measurements and calculations.

We are now developing a finite element blade-to-blade flow calculation in order to produce an automatic, complete quasi-3D solver. Our purpose is again to obtain a low-time-consuming, simple, stable, numerical code in order to use it in an engineering design context.

REFERENCES

1. J. H. Saiac, 'Finite element method for time-dependent Euler equation', *Math. Methods Appl. Sci.*, **5**, 22–39 (1983).
2. J. H. Saiac, 'On numerical solutions of the time-dependent Euler equations for incompressible flow', *Int. j. numer. methods fluids*, **5**, 637–656 (1985).
3. O. Pironneau, 'On the transport diffusion algorithm and its application to the Navier–Stokes equations, *Numer Math.*, **8**, 309–332 (1980).
4. C. Bardos, M. Bercovier and O. Pironneau, 'The vortex method with finite elements', *Math. Comput.*, **36**, 153 (1981).
5. F. El Dabaghi and O. Pironneau, 'Stream vectors in the three dimensional aerodynamics', *Numer. Math.* **48**, 561–589 (1986).
6. F. El Dabaghi and J. H. Saiac, 'Characteristics and time dependent methods for solving the 3D incompressible Euler equations by a stream-vector vorticity formulation', Hydrosoft Computational Mechanics Publications, to appear 1989.

7. W. G. Habashi, in C. Taylor and K. Morgan (eds), *Numerical Methods for Turbomachinery, Recent Advances in Numerical Methods in Fluids*, Pineridge Press, Swansea, 1980.
8. W. G. Habashi and M. M. Hafez, 'Finite element solutions of transonic external and internal flow calculations', *ASME Paper 83-GT-35*, 1983.
9. Ch. Hirsch and G. Warzee, 'A finite element method for through flow calculations in turbomachines', *ASME J. Fluids Eng.*, **98**, 403–421 (1976).
10. R. Glowinski, *Numerical Methods for Nonlinear Variational Problems*, Springer, 1984 pp. 199–206.
11. A. Eydeland, and B. Turkington, 'A computational method of solving free-boundary problems in vortex dynamics,' *J. Comput. Phys.*, **78**, 194–214 (1988).
12. H. Brezis and M. Sibony, 'Methodes d'approximation et d'iteration pour les operateurs monotones', *Arch. Rat. Mech. Anal.* **28**, 59–82 (1968).
13. V. Arnol'd, *Mathematical Methods of Classical Mechanics*, Springer, 1978.